Published in final edited form as:
Cancer Res. 2013 December 1; 73(23): . doi:10.1158/0008-5472.CAN-13-1355.

Glioblastoma stem cells are regulated by interleukin-8 signaling in a tumoral perivascular niche

David W. Infanger[1], **YouJin Cho**[1], **Brina S. Lopez**[2], **Sunish Mohanan**[3], **S. Chris Liu**[1], **Demirkan Gursel**[4], **John A. Boockvar**[4], and **Claudia Fischbach**[1,5]

[1]Department of Biomedical Engineering, Cornell University, Ithaca, New York

[2]Department of Veterinary Medicine, Colorado State University, Fort Collins, Colorado

[3]Department of Comparative Biomedical Sciences, Cornell University, Ithaca, New York

[4]Laboratory for Translational Stem Cell Research, Weill Cornell Brain Tumor Center, Department of Neurological Surgery, Weill Cornell Medical College, New York, New York

[5]Kavli Institute at Cornell for Nanoscale Science, Cornell University, Ithaca, New York

Abstract

Glioblastoma multiforme (GBM) contains a subpopulation of cancer stem-like cells (CSCs) believed to underlie tumorigenesis and therapeutic resistance. Recent studies have localized CSCs in this disease adjacent to endothelial cells (ECs) in what has been termed a perivascular niche, spurring investigation into the role of EC-CSC interactions in GBM pathobiology. However, these studies have been limited by a lack of in vitro models of three-dimensional disease that can recapitulate the relevant conditions of the niche. In this study, we engineered a scaffold-based culture system enabling brain ECs to form vascular networks. Using this system, we demonstrated that vascular assembly induces CSC maintenance and growth in vitro and accelerates tumor growth in vivo through paracrine IL-8 signaling. Relative to conventional monolayers, ECs cultured in this three dimensional system not only secreted enhanced levels of IL-8 but also induced CSCs to upregulate the IL-8 cognate receptors CXCR1 and CXCR2, which collectively enhanced CSC migration, growth and stemness properties. CXCR2 silencing in CSCs abolished the tumor-promoting effects of ECs in vivo, confirming a critical role for this signaling pathway in GMB pathogenesis. Together, our results reveal synergistic interactions between ECs and CSCs that promote the malignant properties of CSCs in an IL-8-dependent manner. Furthermore, our findings underscore the relevance of tissue-engineered cell culture platforms to fully analyze signaling mechanisms in the tumor microenvironment.

Keywords

glioblastoma; interleukin-8; cancer stem cells; microenvironment; tissue engineering

Introduction

Glioblastoma multiforme (GBM), a high grade (IV) astrocytoma, remains the most common and lethal primary brain tumor in adults with a median survival of 12–15 months(1). Clinical management of GBM is largely palliative, due to poor efficacy of conventional therapeutics

Corresponding Author: Dr. Claudia Fischbach-Teschl, Associate Professor, Department of Biomedical Engineering, Cornell University 157 Weill Hall, Ithaca, New York, 14853, Phone (607) 255-4547, Fax (607) 255-7330, cf99@cornell.edu.

Conflicts of Interest: None

and reflexive secondary tumor formation following resection. The identification of GBM-associated “cancer stem cells” (CSC) has fueled research into the contributing role of this cell type in GBM pathogenesis and therapeutic resilience(2). GBM CSCs are capable of self-renewal and multi-lineage differentiation, enable tumorigenesis upon intracranial implantation within immunocompromised rodents(3), and exhibit elevated therapeutic resistance relative to bulk glioma cells(4). Therefore, elucidation of the molecular mechanisms underlying CSC maintenance and proliferation in the tumor microenvironment offers new focus toward the development of improved anti-GBM therapies.

Cell-microenvironment interactions modulate GBM pathogenesis, whereby perivascular localities are particularly important as they support the malignant behavior of CSCs(5, 6). Specifically, association with endothelial cells (ECs) or capillary structures supports maintenance of Nestin+ and CD133+ CSCs by sustaining their undifferentiated state and proliferation(5). Likewise, paracrine signaling by CSCs enhances the apoptotic threshold of ECs(7), thereby preserving the perivascular microenvironment necessary for downstream processes involved in GBM pathology. Nevertheless, despite accumulating evidence confirming the importance of CSC-EC signaling in GBM pathogenesis, the precise molecular mechanisms involved in CSC localization to – and function within - the perivascular niche remain poorly defined.

Interleukin-8 (IL-8) has received significant attention as a pro-migratory and pro-angiogenic stimulus in multiple cancers, but may regulate GBM-CSC functions as well(8). The effects of the ~8 kDa chemokine are mediated via binding to either of two related G protein-coupled receptors, CXCR1 and CXCR2, whose expression varies dramatically by cell type and throughout pathogenesis(9). While initially identified as a monocyte-secreted chemotactic factor for neutro/basophils and T-lymphocytes, IL-8 can similarly facilitate invasion of bulk glioma cells and has been associated with increased tumor grade in astrocytic neoplasms(10, 11). In addition to its direct pro-angiogenic effects, IL-8 can promote GBM tumor vascularization indirectly by elevating the apoptotic threshold of ECs as well as promoting expression of matrix-remodeling enzymes necessary for endothelial sprouting(9, 12). Although it has been recently revealed that autocrine IL-8 signaling contributes to CSC self-renewal within other tumors of the breast and liver(13, 14), its impacts on the behavior of GBM CSCs, signaling with ECs of the perivascular niche, and participation in GBM tumor growth have yet to be elucidated.

IL-8 expression and secretion are heavily influenced by 3-D cell-microenvironment interactions(15, 16), underscoring the importance of physiologically relevant, three-dimensional (3-D) culture models to study IL-8 signaling as it relates to human CSCs and ECs throughout GBM pathogenesis. We have previously shown that tissue-engineered 3-D culture systems mimic *in vivo*-like IL-8 expression by recapitulating appropriate microenvironmental conditions including cell-cell and cell-extracellular matrix interactions(15, 16). Here, we utilized porous, polymeric scaffolds as platforms to investigate the role of paracrine EC signaling on patient-derived GBM-CSC pathogenesis *in vitro* and *in vivo*. Our findings indicate that IL-8 serves as a critical mediator supporting CSC growth and migration toward ECs, which may partially explain their perivascular co-localization in the GBM tumor microenvironment, thereby offering promise as a novel therapeutic target for the clinical management of the disease. Furthermore, these studies undrescore the importance of appropriate culture systems in studying tumor-stroma interactions and support that tissue-engineered models are suitable to evaluate microenvironmentally regulated paracrine signaling *in vitro* and *in vivo*.

Materials and Methods

Cell Culture

Immortalized human brain ECs (hCMEC, provided by Dr. Babette Weksler, Weill Cornell Medical College(17)) were cultured on collagen-coated (1%) flasks in Clontecs EGM-2 media (Lonza). Patient-derived GBM stem cells (CSCs, provided by Dr. John Boockvar, Weill Cornell Medical College) were isolated from GBM tumor specimens (WHO grade IV) as described previously(18). Briefly, GBM tissue was digested in PBS containing papain (Worthington) and DNAse 1 (Sigma-Aldrich), then titurated via pipette and filtered through a 70μm sterile cell filter (BD Biosciences). Cells were resuspended in stem cell media containing 1:1 Dulbecco's Modified Eagle's Medium:F12 (Gibco) plus basic FGF and EGF (each 20ng/mL, Invitrogen) and 1x antibiotic/anti-mycotic (Gibco). An isolated cell was clonally expanded in non-adherent culture flasks and media changed every 48–72 hours, resulting in neurosphere aggregates. Two GBM CSC cell populations, labeled CSC 248(EGFR+/PTEN+) and CSC 974 (EGFR+/PTEN-), were utilized. Expression of stem cell markers Nestin, Sox2, Oct4, and Musashi-1, GFAP, and Bim-1 and absence of Olig-1, Tuj-1, and NeuN were verified via immunocytochemistry, and tumorigenicity confirmed via implantation into athymic mice(18).

Polymeric Scaffold Fabrication and Cell Seeding

Porous, polymeric scaffolds were fabricated using a gas-foaming, particulate leaching method(19). Briefly, poly(lactide-co-glycolide) (PLG) particles (Lakeshore Biomaterials, ground and sieved to ~250μm diameter), PLG microspheres (formed via double emulsion, ~5–50μm diameter), and sodium chloride (J.T. Baker, sieved to ~250–400μm diameter) were mixed and pressed into matrices (8.5mm diameter, 1mm thick) at room temperature (Carver Press, Fred S. Carver). Polymer-foaming was achieved by exposing matrices to high-pressure (800psi) carbon dioxide and releasing gas quickly using a pressure vessel (Parr Instruments). Subsequently, sodium chloride porogen was leached out with de-ionized water. Scaffolds were sanitized in 70% ethanol and washed in sterile PBS. $1.5E^6$ hCMEC, $1.0E^5$ CSC, or both cell types (aforementioned cell densities) were suspended in 30μL of 1:1 (media:Matrigel, BD Biosciences) and slowly pipetted onto the scaffold. Following 30 minutes of incubation at 37C (to allow cell permeation), scaffolds were placed on ice until implantation. Alternatively, media was to scaffolds under dynamic conditions using an orbital shaker for *in vitro* experiments.

Animal Studies

Animal studies were performed according to approved protocols by the Cornell University Animal Care and Use Committee. Male, 6–8 week old, CB17 SCID mice (Charles River Labs) were anesthetized and incisions made to the dorsal infrascapular skin. A subcutaneous pocket was created, irrigated with sterile PBS, cell-seeded PLG scaffolds (described above) inserted, and then sutured with 5-0 Ethilon (Ethicon). Studies investigating *in vivo* polymer degradation used blank sanitized scaffolds. High-resolution ultrasound imaging was performed weekly using the VEVO 770 Imaging system and RMV 706 single-element transducer (Visualsonics). Mice were anesthetized (1.5% isoflurane) and implantation site hair removed by chemical debridement (Nair, Church & Dwight Co). Mice were placed prone on a heated stage and scaffolds imaged with semi-automated 3-D, B-mode imaging at 40MHz frequency. To calculate tumor volume, cross-sectional areas of PLG scaffold+tumor were determined and then integrated to measure total volume, using VEVO software (v. 3.0.0).

Immunostaining and histology

CSC neurospheres cultured in non-adherent flasks were collected by centrifugation and embedded in OCT (Tissue-Tek) in minimal PBS following washing, fixation with 4% paraformaldehyde (PFA) and incubation in 20% sucrose/PBS. After cryosectioning (14μm), immunostaining was performed on Triton-X (VWR, 0.5%) permeabilized cells with antibodies against human Sox-2 (Sigma), Oct-4 (Millipore), Nestin (Millipore) or control rabbit/mouse IgG (Invitrogen) at 1:200 dilution. Secondary antibodies (1:500, anti-rabbit Alexafluor 488 or anti-mouse Alexafluor 546, Invitrogen) were diluted in PBS containing 4', 6-diamidino-2-phenylindole (DAPI) (1:5000) for nuclear counterstain; imaging was performed on a Zeiss LSM 710 confocal microscope.

For *in vivo* studies, tumors were removed and fixed overnight in 4% PFA, then bifurcated and half submitted for paraffin sectioning (4μm) and subsequent H&E staining; remaining half was immersed in 20% sucrose/PBS overnight, embedded in OCT, and cryosectioned (14μm). Immunostaining was performed as above to detect stem cell marker levels; in addition, species-specific EC marker CD31 was probed (mouse anti-human, Invitrogen; rat anti-mouse, BD Pharmingen) at 1:200 dilution, followed by secondary Alexafluor 546 (goat anti-mouse) or Alexafluor 647 (goat anti-rat) antibody at 1:500 (both from Invitrogen). Sections were counterstained with DAPI (1:5000) and imaged on a Zeiss LSM 710 confocal microscope.

Conditioned Media Preparation

hCMEC-seeded PLG scaffolds were cultured for 3 days, after which EGM-2 media was removed, scaffolds washed in sterile PBS, and basal EBM-2 media (sans growth supplements, with 0.25% FBS and 0.1% penicillin/streptomycin) added. Media was collected at 24 hours and IL-8 ELISA (R&D systems) performed per manufacturer's instructions. Subsequently, media was concentrated 10x at 4C using Amicon Ultrafree 15 centrifugal filter units (3000 MWCO, Millipore). Concentrated media (termed "3-D EC-conditioned medium") was normalized to DNA content, as determined by fluorimetric DNA assay (Quantifluor assay, Promega) of scaffold lysates in Caron's buffer. To generate 2-D-conditioned EC medium, hCMECs were cultured as sub-confluent monolayers and media collected, concentrated, and normalized to like DNA concentrations as above described for 3-D conditioned media. Basal control medium was generated by incubating basal EBM-2 media for 24 hours at 37C and concentrating 10-fold as above described. Prior to use, conditioned media were diluted to 2x final concentration in stem cell medium and supplemented to CSC cultures for three days of preconditioning prior to subsequent analyses.

Conditioned CSC medium was created by culturing CSCs in non-adherent flasks until neurospheres of ~100μm formed, at which point media was replaced with fresh stem cell medium lacking antibiotics. Media was then concentrated and normalized to DNA content as above described.

Transwell Migration Assay

Transwell inserts (Falcon HTS FluroBlok Inserts, 8μm pore size) were coated with 1% collagen I (BD Biosciences), washed, and placed in 24-well plates. Dissociated CSCs (10,000; with or without prior preconditioning in 3-D EC-conditioned media) were added to each Transwell in 300μL stem cell media and migration assessed following addition of recombinant human IL-8 or IgG (50 or 5ng/mL, Genescript) to stem cell media in the lower compartment. Alternatively, migration towards EC-secreted factors was determined by adding 300μL medium composed of equal parts stem cell medium and either 10× 3-D EC medium or 10x basal EC medium. To confirm the role of IL-8 in CSC chemotaxis,

antagonist antibodies to human IL-8 (7.5 μg/mL), CXCR1 (2 μg/mL), or CXCR2 (2 μg/mL, all from R&D Systems) were added prior to the start of the experiment (anti-IL-8 added to medium; anti-CXCR1/2 added to cells+medium for 1 hour at RT prior to experiment). After 16 hours, Transwells were fixed in 4% PFA and DAPI stained (1:5000). Transwell underside images were collected at 10x on a Zeiss Observer Z.1 microscope fitted with an AxioCam MRN camera. For each of triplicate experiments, the average number of migrated cells from 7 random images/well from 4 wells was calculated using ImageJ software (NIH).

Cell growth in response to IL-8 stimulation

Freshly-dissociated CSCs were placed in non-adherent plates (30,000/12-well) in stem cell medium. IL-8 supplementation (50ng/mL, Genescript) alone or with antibody antagonists to IL-8, CXCR1, or CXCR2 (dosages and pre-incubation as above for Transwell studies) was provided at the start of the experiment and at 24 hours. After 48 hours, cells were collected by brief centrifugation and DNA assay performed on Caron's buffer-treated cell lysates as above described. Data are represented as normalized values relative to CSC cultures without IL-8 treatment.

Real Time RT PCR and shRNA-mediated CXCR2 gene knockdown

Following 3 days of preconditioning in 3-D-conditioned or basal media, total RNA from CSC neurospheres was harvested with TRIzol (Invitrogen) according to manufacturer's instructions and 1μg reverse-transcribed to cDNA (qScript cDNA supermix, Quanta BioSciences) using random hexamer and oligo(dt) primers. Real-time, RT PCR was performed on 25ng template using SYBR green detection (Quanta Biosciences) and an Applied Biosystems 7500 System. Primer sequences (300nM, IDT Technologies) were as follows: human CXCR1 (fwd: 5'tcaagtgccctctagctgtt3', rev: 5'gggctgtaatcttcatctgc3'); human CXCR2 (fwd: 5'agaagtttcgccatggactcctca3', rev: 5'agtggaagtgtgccctgaagaaga3') and β-actin loading control (fwd: 5'aatgtggccgaggactttgattgc3', rev: 5'aggatggcaagggacttcctgtaa3'). Relative quantification was performed using the $\Delta\Delta C_t$ method(20).

To establish long-term knockdown of CXCR2 expression, lentiviruses encoding shRNA sequences targeted against human CXCR2 or random shRNA sequence (MISSION shRNA lentiviral transduction particles, Sigma Aldrich) were transduced at 5 MOI to $1E^4$ GBM CSCs in a 12-well dish overnight, rinsed with sterile PBS, and transferred to stem cell medium. CXCR2 knockdown of 70% (vs. control transduced) was confirmed by real time RT PCR when three CXCR2-specific shRNA lentiviruses were used concurrently (TRCN0000009136, TRCN0000009137, TRCN0000009138, Sigma-Aldrich). Additionally, CXCR2 knockdown was confirmed at the protein level using Western Blot analysis. CSCs previously transduced with siRNA-control or siRNA-expressing lentiviruses were centrifuged and harvested at 4C in RIPA buffer containing protease and phosphatase inhibitors (Roche). Protein concentrations were assessed by BCA assay (Pierce), 50μg separated on a pre-cast 10% polyacrylamide gel (Bio-Rad), and then transferred to a PVDF membrane (Bio-Rad). Membranes were blocked with 5% non-fat dry milk for 1 hour, then probed with mouse anti-human CXCR-2 (R&D systems, 1:200) and α-tubulin (Genscript, 1:5000) antibodies followed by goat anti-mouse HRP secondary antibodies. Densitometric analysis of bands was performed with ImageJ (NIH).

Statistical Analysis

All experiments were performed three separate times and data reported as mean ± SD. One-way analysis of variance (ANOVA) followed by the Tukey post-test were performed to conclude statistical significance, with $\alpha=0.05$, using Prism 5 software (Graphpad).

Results

In vivo tumor formation by CSC-seeded 3-D polymeric scaffolds recapitulates clinical features of human GBM and is accelerated by EC signaling

To study the contributions of the 3-D microenvironment and EC signaling on CSC behavior, CSCs from patient GBM resections were utilized. These cells were cultured in non-adherent flasks under typical stem cell culture conditions over multiple passages and formed characteristic neurospheres that robustly expressed stem cell markers Sox2, Nestin, and Oct4 (Fig. 1A) and were capable of multi-lineage differentiation under serum-containing conditions (Supplemental Fig. S1). Using this undifferentiated CSC population, we first wanted to confirm that co-implantation of human CSCs with human brain ECs (hCMECs) within highly porous PLG scaffolds enhances GBM formation relative to that of CSCs alone. Indeed, longitudinal measurements of tumor and scaffold volumes via high-resolution ultrasound demonstrated that CSCs implanted together with hCMECs exhibited significantly accelerated tumor formation as compared to CSCs alone by 8–11 weeks (Fig. 1B). Since blank control scaffolds were largely degraded (~80%) by six weeks, final tumor volumes were due to differences in cell number rather than scaffold contributions (Fig. 1C). Furthermore, ultrasound analysis revealed multiple regions of blood flow throughout the mass suggesting that neoplasms derived from co-implantation were highly vascularized (Supplemental Fig. S2A), which is consistent with human GBM.

Following explantation, tumors were subjected to histological analysis to confirm that the subcutaneous PLG implantation model mimicked bona fide GBM. Evaluation of H&E-stained cross-sections demonstrated that tumors contained extensive necrotic cores, which were circumscribed by large pseudo-palisading nuclei (Fig. 1D), both considered clinical markers of human GBM (21). Furthermore, frequent microvascular hyperplasia (Supplemental Fig. S2B), along with common detection of mitotic figures (Supplemental Fig. S2C) and diffuse tumor cell infiltration outside of the primary tumor mass (Supplemental Fig. S2D) further supported the diagnosis of a grade IV malignant glioma(22). To further identify the fate of the implanted ECs and assess whether CSCs maintained preferential perivascular co-localization as reported in clinical specimens (5) we performed immunohistochemical analysis of endothelial and CSC markers. Similar to previous results with human dermal microvascular ECs(23), hCMECs formed capillary structures that anastomosed with the mouse vasculature (Fig. 1E, Supplemental Figure S3A). Similarly, these vessels borne from co-implantation appeared larger than those observed in tumors formed from by CSC implantation alone; however, the extent of tumor vascularization was similar between both groups (Supplemental Figure S3B). Interestingly, $Sox2^+$ (Fig. 1F) and $Oct4^+$ (Supplemental Fig. S3C) CSCs were detected largely in close or direct proximity to these capillary structures and associated more frequently with portions of the vessels that contained human ECs (Fig. 1F) suggesting the establishment of perivascular niches supportive of CSC maintenance in our model.

3-D microenvironmental conditions stimulate EC secretion of paracrine factors that support CSC functions *in vitro*

To specifically isolate the paracrine signaling effects of hCMECs on CSC-mediated gliomagenesis in our model, we next performed *in vitro* studies in which hCMECs were cultured in PLG scaffolds to recapitulate their 3-D interactions within the vasculature. Cells adhered readily within the pores of the scaffolds and arranged into capillary tube-like structures that matured over sustained culture periods (Fig. 2A), demonstrating the ability of our model to support 3-D vasculogenic processes and microenvironmental conditions *in vitro*. To evaluate if scaffold culture and, thus, 3-D microenvironmental context, affected the ability of hCMECs to modulate CSC functions, we performed conditioned media

experiments. To this end, conditioned media from hCMECs cultured in conventional 2-D culture or 3-D PLG scaffolds was collected and supplemented to CSC cultures (Fig. 2B). Paracrine factors from 3-D hCMECs were significantly more efficacious in retaining expression of CSC stem cell markers Nestin and Sox2 than conditioned media from 2-D hCMEC cultures or basal medium, where Sox2 expression was minimal and Nestin expression nearly absent (Figs. 2C–D). Furthermore, 3-D-derived hCMEC signaling factors also accelerated CSC growth *in vitro*. This was evidenced by larger neurosphere size in cultures supplemented with media from 3-D-cultured hCMECs, which was further corroborated by an almost 3-fold increase in total DNA relative to similar cultures fortified with conditioned media from 2-D hCMEC cultures (Fig 2E). In light of the heterogeneous stem cell marker expression, cultures supplemented with 2-D conditioned media likely contain a mixed population of CSCs (Fig. 2C) making the differences in neurosphere area and DNA content seem even more dramatic. This was substantiated by the presence of frequent plate adhesion of glial-like cells in CSC cultures receiving 2-D conditioned media, which was nearly absent in similar cultures fortified with 3-D factors (Supplemental Fig. S4). Collectively, these data suggest that 3-D microenvironmental conditions play a pivotal role in mediating paracrine signaling by hCMECs which support CSC maintenance and growth.

Interleukin-8 regulates the migration and growth of GBM CSCs

Three-dimensional culture conditions can increase IL-8 expression and secretion in various 3-D culture formats (15, 19, 24). Furthermore, IL-8 reportedly plays important roles in GBM angiogenesis (9), glioma and tumor-associated EC motility (11, 25), and non-GBM CSCs self-renewal and pluripotency (13, 14). Therefore, we next hypothesized that greater CSC growth and maintenance in response to 3-D hCMEC-conditioned media may be related to elevated IL-8 availability. Indeed, 3-D cultured hCMECs secreted significantly more IL-8 relative to the same number of cells maintained in 2-D monolayers (Fig. 3A). Interestingly, exposure of 3-D hCMEC cultures to soluble factors secreted by CSCs further enhanced IL-8 secretion by these cells. Together, these data demonstrate a supportive role for 3-D cell-microenvironment interactions on EC-derived IL-8 concentrations within the perivascular microenvironment (Fig. 3A).

To better define the direct contributions of IL-8 to CSC migration and growth (i.e., two parameters regulating CSC recruitment to and maintenance within the perivascular niche), we performed studies with recombinant human IL-8. The chemotactic ability of IL-8 on CSCs was assessed with a Transwell migration assay using two separate, patient-derived CSC populations. In both cases, IL-8 increased migration of CSCs 5- to 10-fold from control groups challenged with control media (Fig. 3B), which was preserved to a lesser, yet significant, extent with a 10-fold reduction in IL-8 concentration (Supplemental Figure S5A). To analyze whether IL-8 stimulation similarly accelerates CSC growth, patient-derived GBM CSCs were cultured in typical stem cell medium in the presence or absence of human IL-8. Addition of IL-8 elicited a dose-dependent increase in neurosphere size of CSCs, which plateaued at 50ng/mL (data not shown) (Fig. 3C). To confirm that this effect was mediated via binding to the cognate IL-8 receptors CXCR1 and/or CXCR2(9), CSCs were incubated with the respective antagonist antibodies prior to IL-8 treatment. CXCR1 blockade abolished IL-8-induced proliferation and resulted in CSC growth, which matched that of control cultures, suggesting that this receptor is partly responsible for the proliferative effects of IL-8 on CSCs (Fig. 3C). Interestingly, selective impairment of CXCR2 binding more dramatically impacted CSC growth: cell numbers dropped below controls and even below cell numbers at the start of the experiment (data not shown). This indicates that (i) signaling via this receptor is necessary for normal CSC viability and (ii) CSC functions may partly depend on autocrine IL-8 signaling (Fig. 3C). To confirm the

functionalization of IL-8 on CSC growth, saturating levels of an antagonist IL-8 antibody were introduced into cultures that were concomitantly stimulated with IL-8. Again, CSC numbers decreased to levels observed with CXCR2 blockade, further supporting that IL-8 signaling is necessary for both maintenance and proliferation of GBM CSCs (Fig. 3C).

Paracrine communication between brain ECs and CSCs enhances IL-8 signaling and facilitates CSC migration and growth *in vitro*

Next, we sought to determine the functional consequence of the above-mentioned results by evaluating whether 3-D-cultured hCMECs promote CSC migration and growth due to elevated IL-8 signaling. Toward this end, we first broadly compared CSC migration towards 3-D hCMEC-conditioned media, IL-8-fortified, or control basal media using Transwell migration assays. Our results indicated that paracrine factors secreted by scaffold-cultured hCMECs enhanced CSC migration in a similar manner as recombinant IL-8 (2.7- vs. 1.9-fold relative to control conditions). To further determine if chronic signaling by ECs as present in the brain perivascular microenvironment impacts the migratory potential of CSCs, CSCs were pre-conditioned with 3-D hCMEC-secreted factors prior to migration experiments. While this pre-exposure enhanced the overall migratory potential of CSCs only insignificantly, a much more pronounced effect was detected for directed migration towards either 3-D hCMEC conditioned media or IL-8 (Fig. 3D). As these results suggested that hCMEC-derived paracrine signaling factors elevated IL-8 responsiveness, we hypothesized that enhanced migration of pre-conditioned CSCs to IL-8 may be related to altered expression of the cognate receptors CXCR1 and/or CXCR2. Indeed, qPCR analysis of receptor expression for multiple patient-derived GBM CSCs revealed that pre-conditioning of these cells with 3-D hCMEC conditioned media resulted in a 20- and 40-fold increase in CSC CXCR1 and CXCR2 expression, respectively (Fig 3E; CSC 248 population). Importantly, preconditioning with 3-D hCMEC-derived factors only affected CSC expression of IL-8 receptors significantly; intrinsic expression of IL-8 was also downregulated, but these levels were statistically indifferent from 2-D hCMEC-treated cells (Supplemental Fig. S5B). Taken together, these findings demonstrate that synergistic paracrine interactions between brain ECs and GBM CSCs culminate in enhanced IL-8 signaling via cell-specific up-regulation of both ligand (in hCMECs) and its cognate receptors (in CSCs).

While these findings support EC paracrine signaling as an underlying cause of enhanced CSC invasion, they do not directly evaluate participatory roles of IL-8 or CXCR-1/CXCR-2 in this process. Therefore, to directly assess the contributions of IL-8 stimulation and/or CXCR1/2 binding on cell migration, antagonist antibodies to each were incorporated in repeat Transwell assays. Selective inhibition of IL-8 in 3-D-conditioned hCMEC media, strongly decreased migration of pre-conditioned GBM CSCs, thereby demonstrating that signaling cascades initiated by this factor are pivotal to CSC chemotaxis (Fig. 3F). Likewise, when cells were treated with antagonists to either CXCR1 or CXCR2, CSC migration was similarly attenuated, establishing that signaling through both receptors functions to facilitate CSC migration. Interestingly, CXCR2 inhibition appeared to have a greater impact on CSC invasion than did CXCR-1 blockade, yet these results were not statistically significant. Importantly, the impact of these antagonist antibodies was specific to IL-8 signaling, as treatment with IgG control antibody elicited no effect on CSC migration (Supplemental figure S5C). These data implicate both receptors in CSC migration towards EC-secreted IL-8 within the perivascular microenvironment.

Lastly, the functional significance of 3-D hCMEC-mediated CXCR1 and CXCR2 upregulation on CSC growth was evaluated. To this end, pre-conditioned CSCs were cultured in the presence or absence of selective antagonists to IL-8 or its cognate receptors. Similar to the migration findings above, blockade of either receptor significantly impaired

the effects of pre-conditioning on CSC growth (Fig. 3F). Similarly, direct blockade of IL-8 also impaired the effects of preconditioning with 3-D hCMEC-derived factors on CSC proliferation, further implicating that the stimulatory effects of paracrine EC signaling on CSC growth are mediated through IL-8 binding to both CXCR1 and CXCR2.

Inhibition of CXCR2 signaling by CSCs abolishes the stimulatory effects of ECs on tumor growth *in vivo*

Thus far, these results provide corroborating evidence that IL-8 signaling is a critical mediator of GBM CSC migration, maintenance, and growth. Therefore, to directly assess whether IL-8 receptor signaling in GBM CSCs underlies tumor formation siRNA-based inhibition strategies were used. Given the more pronounced effect of CXCR2 in IL-8-mediated CSC growth (Fig. 3C), siRNA sequences targeted against human CXCR-2 were generated and incorporated into lentiviruses to stably knock-down expression of this receptor (Supplemental Fig. S6A). Co-transduction of three constructs in GBM CSCs caused a robust (~80%, Supplemental Fig. S6B) knockdown of CXCR2 expression and protein levels (~65%, Supplemental Figure S6C) with no impact on expression of CXCR1 (data not shown). Next, transduced or native cells were seeded alone or in combination with hCMECs in PLG scaffolds, which were then subcutaneously implanted in SCID mice. Co-implantation of native CSCs with hCMECs recapitulated prominent tumor formation by 8 weeks, whose volume dramatically exceeded that of tumors borne by CSC implantation alone (Fig. 4A, B). However, these effects were abolished with CXCR2 knockdown, whereby the volume of tumors formed by transduced GBM CSCs was half that of those generated by native CSCs (Fig. 4B). Despite this difference in size, these tumors were vascularized to a similar extent as those resulting from native CSC implantation (Supplementary Fig. S7), supporting that differences in tumor growth were not merely the result of stunted tumor perfusion. Importantly, co-implantation of hCMECs with CXCR2 knocked-down CSCs failed to reverse these effects or accelerate tumor formation (Fig. 4B), thus providing strong evidence that the promoting effects of brain ECs on GBM CSC-dependent tumor growth are mediated in large part through CXCR2 signaling.

Discussion

Delineating the signaling pathways that regulate CSC maintenance, proliferation, and tumorigenicity in the perivascular niche have proved challenging due to a paucity of *in vitro* models which faithfully recapitulate 3-D microenvironmental conditions. In this study, we utilized a scaffold-based culture system that enables brain ECs to form vascular networks, thereby initiating paracrine IL-8 signaling cascades, which enhance CSC maintenance and growth *in vitro* and tumor formation *in vivo*.

The detected upregulation of IL-8 in our studies may have been caused by a variety of microenvironmental conditions including altered dimensionality(15), direct cell-cell contact(26), and cell-ECM interactions(27). Furthermore, varied intraculture oxygen-concentrations could have been involved(28), whereby this response is regulated by changes in cell morphology that may result from varied culture dimensionality(29), as well as pathological consequences of cell death (e.g., necrosis)(30). Moreover, reciprocal interactions between various GBM-associated cell types modulate this response. For example, GBM-associated ECs exhibit enhanced expression of IL-8(31). Accordingly, hCMECs pre-exposed to conditioned media from GBM CSCs increased IL-8 production in our studies (Fig. 3A), suggesting that CSC-derived signaling is partly responsible for the altered gene expression observed in GBM-derived primary ECs(31). It is unknown whether the concentrations of IL-8 secreted by ECs in our study are sufficient to effect CSC functions as we observed, given that these latter experiments were performed using a

considerably higher IL-8 stimulus. However, ECM in the tumor microenvironment can function indirectly to enhance local IL-8 concentrations to levels that approach those used in our studies. For example, components of the ECM such as heparin and heparan sulfate can efficiently bind IL-8 via its heparin-binding domains(32) thereby creating signaling depots which contribute to enhanced cell chemotaxis(33). Future quantitative analysis of spatial differences in IL-8 from ex vivo tumor samples would help to evaluate this possibility.

Culture context-driven endothelial upregulation of IL-8 directly affected CSC maintenance and growth, which was further enhanced by CSC pre-conditioning with media from 3-D EC cultures. Specifically, chronic exposure of CSCs to EC signals as would occur in the perivascular microenvironment upregulated the IL-8 receptors CXCR1 and CXCR2, with functional consequences of enhanced CSC migration and growth. Interestingly, other interleukin receptors have previously been associated with GBM CSC malignancy. More specifically, GBM CSCs express elevated levels of the interleukin 6 (IL-6) receptors IL6Rα and glycoprotein 130 (gp130) relative to non-stem glioma cells, which promotes their self-renewal and tumorigenic capability(34). Given that the respective ligands for these receptors (i.e., IL-6 and IL-8) are regulated by the same transcription factors (i.e., nuclear factor-kappaB [NF-kB] and NF-IL6)(35), it is possible that IL-6 secretion by 3-D cultured ECs may partially contribute to altered CSC functions in our studies. Alternatively, IL-6 may serve as an upstream stimulus for the increased transcription of IL-8(36). Hence, it is conceivable that CSC-derived IL-6 not only promotes gliomagenesis in an autocrine manner(34), but also by stimulating the transcription of IL-8 by brain ECs (Fig. 3A).

We have shown that both cognate receptors CXCR1 and CXCR2 participate in the growth- and migratory-inducing effects of IL-8 on CSCs. These findings agree with observations in human microvascular ECs, where blockade of either receptor attenuated chemotaxis towards IL-8(37). However, with regards to cell growth, our data indicate a far greater impact of CXCR2 blockade, which resulted in declining cell counts below control culture levels (Fig. 3C). This may be partially explained by the broader range of signaling molecules, which can bind to this receptor(9). Alternatively, the specific downstream effectors of CXCR2 may be critical to IL-8-induced CSC growth. Included in these are activation of phosphoinositide 3-kinase (PI-3K) and extracellular signal-regulated kinase (ERK) 1/2(38), which have been implicated in the proliferation and differentiation of neural stem cells(39), respectively. Interestingly, PTEN has also been shown to be a potent regulator of PI-3K signaling and has been implicated in the maintenance of various cancer stem cell types (40, 41). However, in our studies both $PTEN^{+}$ and $PTEN^{-}$ CSCs responded similarly to 3-D EC conditioned media (Fig. 2C), suggesting that CXCR2-mediated signaling may invoke similar signaling pathways as PTEN, possibly through PI-3K activation.

While this study was specifically designed to better define the role of EC-derived soluble factors on CSC functions the presented culture model may be broadly applicable to other questions of GBM perivascular niche interactions. For example, CSCs may promote tumor growth by modulating blood vessel functions through differentiation into ECs(42) or pericytes(43). Future studies involving direct co-culture of both cell types within the presented scaffold system may help to better define the underlying molecular and cellular mechanisms and assess whether altered IL-8 signaling may contribute to these changes. Furthermore, the composition and mechanical properties of EC-deposited ECM likely play key roles in guiding CSC, but were not considered in the current study. ECs assemble an ECM that is enriched in laminin a2, a promotor of CSC malignancy(44). As both laminin a2 and IL-8 inversely correlate with patient survival(44, 45) and are upregulated in GBM-associated ECs relative to normal brain ECs(25, 44) it is provocative to consider that a functional link between these two factors exists. Finally, ECM mechanical properties not only critically impact glioma migration(46) and EC behavior(47), but also amplify cellular

response to soluble signals(48). Modulating the presentation of biomaterials within these cell culture platforms would allow evaluation of the collective contributions of these parameters on CSC behavior, which would significantly advance our understanding of the physicochemical parameters influencing cell behavior in the perivascular niche. Finally, it is essential to realize that ECs are not the sole source of IL-8 in the GBM microenvironment. For example, additional cell types resident within the tumor parenchyma, including astrocytes(49) and bulk glioma cells themselves(50) can contribute to interstitial IL-8 levels. Future studies utilizing the 3-D culture platform with these additional cell types would help to elucidate whether paracrine factors secreted by these cell types can similarly enhance CSC sensitivity to IL-8 via receptor upregulation as ECs do.

It is critical to note that while subcutaneous co-implantation of CSCs with ECs mimicked certain GBM-like characteristics *in vivo*, CSCs implanted alone failed to recapitulate advanced tumors within the timespan of the experiment (11 weeks). These findings appear in contrast with other animal models of GBM, e.g., intracranial CSC implantation, which demonstrate rapid tumor formation by these cells, and would thus suggest that additional signaling parameters not afforded by the scaffold model or subcutaneous environment are involved in CSC-mediated tumorigenesis(51). As it is possible that varied vascular density contribute to these differences(52), future studies will be required to evaluate the importance of IL-8 signaling in an orthotopic or transgenic model of GBM.

The finding that inhibition of the CXCR2 signaling pathway in CSCs abolishes tumorigenesis *in vivo* has significant implications for the clinical management of human GBM. It is important to note that additional cytokines - CXCL2, CXCL3, and CXCL5, among others(53) - also bind CXCR2 and as such, may participate in CSC-driven gliomagenesis, which has not been investigated herein. Interestingly, the application of certain anti-cancer treatments such as photodynamic (PDT) or temozolomide (TMZ) therapy in multiple glioma cell lines has been shown to stimulate transcription of many of the CXCR2 agonists (e.g., CXCL2, CXCL3, IL-8)(54, 55) as well as IL-6(54) which could, in theory, support subsequent CSC growth and recurrent tumor formation that is nearly reflexive for human GBM. In light of this, the development and delivery of CXCR2 antagonists in combination with conventional therapeutic approaches may offer a significant advantage for clinical treatment of the disease.

In conclusion, we have developed a tissue-engineered culture model to resolve the impact of 3-D microenvironmental conditions on EC-mediated paracrine signaling, which supports GBM tumor initiation and progression. Our results revealed that perivascular niche-associated IL-8 signaling between endothelial and cancer stem cells may contribute to poor clinical prognosis. These findings not only warrant the future study of anti-CXCR2 therapies for clinical management of GBM, but also underscore the value of physiologically relevant models for the study of patient cancer cell behavior.

Supplementary Material

Refer to Web version on PubMed Central for supplementary material.

Acknowledgments

The authors would like to recognize the contributions and creativity of Dr. Caroline Coffey (posthumous) which provided the basis of many experiments outlined in this study.

Grant Support

This work was supported by NIH/NCI (RC1 CA146065) and the Cornell Center on the Microenvironment & Metastasis through Award Number NCI U54 CA143876, and by an NIH 5K08CA130985-05 (J.A.B). D.W.I. was

funded through an American Brain Tumor Association (ABTA) Basic Research Fellowship on behalf of Team Will Power and a National Cancer Institute/Cornell Nanobiotechnology Center Young Investigator Award. Additionally, Y.C. was supported by a NYSTEM summer research fellowship, and B.S.L was supported by an NIH T35AI007227 training grant. The content is solely the responsibility of the authors and does not necessarily represent the official views of NCI or NIH.

References

1. Buckner JC, Brown PD, O'Neill BP, Meyer FB, Wetmore CJ, Uhm JH. Central nervous system tumors. Mayo Clin Proc. 2007; 82:1271–1286. [PubMed: 17908533]
2. Singh SK, Clarke ID, Terasaki M, Bonn VE, Hawkins C, Squire J, et al. Identification of a cancer stem cell in human brain tumors. Cancer Research. 2003; 63:5821–5828. [PubMed: 14522905]
3. Singh SK, Hawkins C, Clarke ID, Squire JA, Bayani J, Hide T, et al. Identification of human brain tumour initiating cells. Nature. 2004; 432:396–401. [PubMed: 15549107]
4. Bao S, Wu Q, McLendon RE, Hao Y, Shi Q, Hjelmeland AB, et al. Glioma stem cells promote radioresistance by preferential activation of the DNA damage response. Nature. 2006; 444:756–760. [PubMed: 17051156]
5. Calabrese C, Poppleton H, Kocak M, Hogg TL, Fuller C, Hamner B, et al. A perivascular niche for brain tumor stem cells. Cancer Cell. 2007; 11:69–82. [PubMed: 17222791]
6. Lathia JD, Heddleston JM, Venere M, Rich JN. Deadly teamwork: neural cancer stem cells and the tumor microenvironment. Cell Stem Cell. 2011; 8:482–485. [PubMed: 21549324]
7. Brown CK, Khodarev NN, Yu J, Moo-Young T, Labay E, Darga TE, et al. Glioblastoma cells block radiation-induced programmed cell death of endothelial cells. FEBS letters. 2004; 565:167–170. [PubMed: 15135073]
8. Zhu VF, Yang J, Lebrun DG, Li M. Understanding the role of cytokines in Glioblastoma Multiforme pathogenesis. Cancer letters. 2012; 316:139–150. [PubMed: 22075379]
9. Brat DJ, Bellail AC, Van Meir EG. The role of interleukin-8 and its receptors in gliomagenesis and tumoral angiogenesis. Neuro Oncol. 2005; 7:122–133. [PubMed: 15831231]
10. Van Meir E, Ceska M, Effenberger F, Walz A, Grouzmann E, Desbaillets I, et al. Interleukin-8 is produced in neoplastic and infectious diseases of the human central nervous system. Cancer Research. 1992; 52:4297–4305. [PubMed: 1643627]
11. Raychaudhuri B, Vogelbaum MA. IL-8 is a mediator of NF-kappaB induced invasion by gliomas. J Neurooncol. 2011; 101:227–235. [PubMed: 20577780]
12. Li A, Dubey S, Varney ML, Dave BJ, Singh RK. IL-8 directly enhanced endothelial cell survival, proliferation, and matrix metalloproteinases production and regulated angiogenesis. J Immunol. 2003; 170:3369–3376. [PubMed: 12626597]
13. Ginestier C, Liu S, Diebel ME, Korkaya H, Luo M, Brown M, et al. CXCR1 blockade selectively targets human breast cancer stem cells in vitro and in xenografts. The Journal of clinical investigation. 2010; 120:485–497. [PubMed: 20051626]
14. Tang KH, Ma S, Lee TK, Chan YP, Kwan PS, Tong CM, et al. CD133(+) liver tumor-initiating cells promote tumor angiogenesis, growth, and self-renewal through neurotensin/interleukin-8/CXCL1 signaling. Hepatology. 2012; 55:807–820. [PubMed: 21994122]
15. Fischbach C, Chen R, Matsumoto T, Schmelzle T, Brugge JS, Polverini PJ, et al. Engineering tumors with 3D scaffolds. Nat Methods. 2007; 4:855–860. [PubMed: 17767164]
16. Verbridge SS, Choi N, Zheng Y, Brooks DJ, Stroock A, Fischbach-Teschl C. Oxygen-controlled 3-D cultures to analyze tumor angiogenesis. Tissue Eng Part A. 2010
17. Weksler BB, Subileau EA, Perriere N, Charneau P, Holloway K, Leveque M, et al. Blood-brain barrier-specific properties of a human adult brain endothelial cell line. The FASEB journal : official publication of the Federation of American Societies for Experimental Biology. 2005; 19:1872–1874.
18. Howard BM, Gursel DB, Bleau AM, Beyene RT, Holland EC, Boockvar JA. EGFR signaling is differentially activated in patient-derived glioblastoma stem cells. J Exp Ther Oncol. 2010; 8:247–260. [PubMed: 20734923]
19. Pathi SP, Kowalczewski C, Tadipatri R, Fischbach CA. novel 3-D mineralized tumor model to study breast cancer bone metastasis. PLoS One. 2010; 5:e8849. [PubMed: 20107512]

20. Schmittgen TD, Livak KJ. Analyzing real-time PCR data by the comparative C(T) method. Nat Protoc. 2008; 3:1101–1108. [PubMed: 18546601]
21. Brat DJ, Prayson RA, Ryken TC, Olson JJ. Diagnosis of malignant glioma: role of neuropathology. J Neurooncol. 2008; 89:287–311. [PubMed: 18712282]
22. Louis DN, Ohgaki H, Wiestler OD, Cavenee WK, Burger PC, Jouvet A, et al. The 2007 WHO classification of tumours of the central nervous system. Acta Neuropathol. 2007; 114:97–109. [PubMed: 17618441]
23. Nor JE, Peters MC, Christensen JB, Sutorik MM, Linn S, Khan MK, et al. Engineering and characterization of functional human microvessels in immunodeficient mice. Lab Invest. 2001; 81:453–463. [PubMed: 11304564]
24. Verbridge SS, Chandler EM, Fischbach C. Tissue-engineered three-dimensional tumor models to study tumor angiogenesis. Tissue engineering Part A. 2010; 16:2147–2152. [PubMed: 20214471]
25. Charalambous C, Pen LB, Su YS, Milan J, Chen TC, Hofman FM. Interleukin-8 differentially regulates migration of tumor-associated and normal human brain endothelial cells. Cancer Research. 2005; 65:10347–10354. [PubMed: 16288024]
26. Tan CP, Seo BR, Brooks DJ, Chandler EM, Craighead HG, Fischbach C. Parylene peel-off arrays to probe the role of cell-cell interactions in tumour angiogenesis. Integr Biol (Camb). 2009; 1:587–594. [PubMed: 20023775]
27. Fischbach C, Kong HJ, Hsiong SX, Evangelista MB, Yuen W, Mooney DJ. Cancer cell angiogenic capability is regulated by 3D culture and integrin engagement. Proc Natl Acad Sci U S A. 2009; 106:399–404. [PubMed: 19126683]
28. Desbaillets I, Diserens AC, de Tribolet N, Hamou MF, Van Meir EG. Regulation of interleukin-8 expression by reduced oxygen pressure in human glioblastoma. Oncogene. 1999; 18:1447–1456. [PubMed: 10050881]
29. Verbridge SS, Chakrabarti A, Delnero P, Kwee B, Varner JD, Stroock AD, et al. Physicochemical regulation of endothelial sprouting in a 3D microfluidic angiogenesis model. Journal of biomedical materials research Part A. 2013
30. Desbaillets I, Diserens AC, Tribolet N, Hamou MF, Van Meir EG. Upregulation of interleukin 8 by oxygen-deprived cells in glioblastoma suggests a role in leukocyte activation, chemotaxis, and angiogenesis. J Exp Med. 1997; 186:1201–1212. [PubMed: 9334359]
31. Charalambous C, Chen TC, Hofman FM. Characteristics of tumor-associated endothelial cells derived from glioblastoma multiforme. Neurosurg Focus. 2006; 20:E22. [PubMed: 16709028]
32. Kuschert GS, Hoogewerf AJ, Proudfoot AE, Chung CW, Cooke RM, Hubbard RE, et al. Identification of a glycosaminoglycan binding surface on human interleukin-8. Biochemistry. 1998; 37:11193–11201. [PubMed: 9698365]
33. Webb LM, Ehrengruber MU, Clark-Lewis I, Baggiolini M, Rot A. Binding to heparan sulfate or heparin enhances neutrophil responses to interleukin 8. Proceedings of the National Academy of Sciences of the United States of America. 1993; 90:7158–7162. [PubMed: 8346230]
34. Wang H, Lathia JD, Wu Q, Wang J, Li Z, Heddleston JM, et al. Targeting interleukin 6 signaling suppresses glioma stem cell survival and tumor growth. Stem Cells. 2009; 27:2393–2404. [PubMed: 19658188]
35. Matsusaka T, Fujikawa K, Nishio Y, Mukaida N, Matsushima K, Kishimoto T, et al. Transcription factors NF-IL6 and NF-kappa B synergistically activate transcription of the inflammatory cytokines, interleukin 6 and interleukin 8. Proceedings of the National Academy of Sciences of the United States of America. 1993; 90:10193–10197. [PubMed: 8234276]
36. Okamura S, Fujiwara H, Yoneda M, Furutani A, Todo M, Ikai A, et al. Overexpression of IL-6 by Gene Transfer Stimulates IL-8-mediated Invasiveness of KYSE170 Esophageal Carcinoma Cells. Anticancer research. 2013; 33:1483–1489. [PubMed: 23564789]
37. Salcedo R, Resau JH, Halverson D, Hudson EA, Dambach M, Powell D, et al. Differential expression and responsiveness of chemokine receptors (CXCR1-3) by human microvascular endothelial cells and umbilical vein endothelial cells. FASEB journal : official publication of the Federation of American Societies for Experimental Biology. 2000; 14:2055–2064. [PubMed: 11023990]

38. Sotsios Y, Ward SG. Phosphoinositide 3-kinase: a key biochemical signal for cell migration in response to chemokines. Immunol Rev. 2000; 177:217–235. [PubMed: 11138779]
39. Ma DK, Ponnusamy K, Song MR, Ming GL, Song H. Molecular genetic analysis of FGFR1 signalling reveals distinct roles of MAPK and PLCgamma1 activation for self-renewal of adult neural stem cells. Mol Brain. 2009; 2:16. [PubMed: 19505325]
40. Boontheekul T, Hill EE, Kong HJ, Mooney DJ. Regulating myoblast phenotype through controlled gel stiffness and degradation. Tissue engineering. 2007; 13:1431–1442. [PubMed: 17561804]
41. Huang FF, Wu DS, Zhang L, Yu YH, Yuan XY, Li WJ, et al. Inactivation of PTEN increases ABCG2 expression and the side population through the PI3K/Akt pathway in adult acute leukemia. Cancer letters. 2013; 336:96–105. [PubMed: 23603434]
42. Ricci-Vitiani L, Pallini R, Biffoni M, Todaro M, Invernici G, Cenci T, et al. Tumour vascularization via endothelial differentiation of glioblastoma stem-like cells. Nature. 2010; 468:824–828. [PubMed: 21102434]
43. Cheng L, Huang Z, Zhou W, Wu Q, Donnola S, Liu JK, et al. Glioblastoma stem cells generate vascular pericytes to support vessel function and tumor growth. Cell. 2013; 153:139–152. [PubMed: 23540695]
44. Lathia JD, Li M, Hall PE, Gallagher J, Hale JS, Wu Q, et al. Laminin alpha 2 enables glioblastoma stem cell growth. Ann Neurol. 2012; 72:766–778. [PubMed: 23280793]
45. Institute, NC. [Accessed 2013 April 30] REMBRANDT home page. 2005. http://rembrandt.nci.nih.gov. Search string IL8 and Kaplan-Meier survival plot.
46. Pathak A, Kumar S. Independent regulation of tumor cell migration by matrix stiffness and confinement. Proceedings of the National Academy of Sciences of the United States of America. 2012; 109:10334–10339. [PubMed: 22689955]
47. Mammoto A, Connor KM, Mammoto T, Yung CW, Huh D, Aderman CM, et al. A mechanosensitive transcriptional mechanism that controls angiogenesis. Nature. 2009; 457:1103–1108. [PubMed: 19242469]
48. Chandler EM, Seo BR, Califano JP, Andresen Eguiluz RC, Lee JS, Yoon CJ, et al. Implanted adipose progenitor cells as physicochemical regulators of breast cancer. Proceedings of the National Academy of Sciences of the United States of America. 2012; 109:9786–9791. [PubMed: 22665775]
49. Shah A, Silverstein PS, Singh DP, Kumar A. Involvement of metabotropic glutamate receptor 5, AKT/PI3K signaling and NF-kappaB pathway in methamphetamine-mediated increase in IL-6 and IL-8 expression in astrocytes. J Neuroinflammation. 2012; 9:52. [PubMed: 22420994]
50. Dwyer J, Hebda JK, Le Guelte A, Galan-Moya EM, Smith SS, Azzi S, et al. Glioblastoma cell-secreted interleukin-8 induces brain endothelial cell permeability via CXCR2. PLoS One. 2012; 7:e45562. [PubMed: 23029099]
51. Lathia JD, Gallagher J, Myers JT, Li M, Vasanji A, McLendon RE, et al. Direct in vivo evidence for tumor propagation by glioblastoma cancer stem cells. PLoS One. 2011; 6:e24807. [PubMed: 21961046]
52. Fukumura D, Yuan F, Monsky WL, Chen Y, Jain RK. Effect of host microenvironment on the microcirculation of human colon adenocarcinoma. The American journal of pathology. 1997; 151:679–688. [PubMed: 9284816]
53. Ahuja SK, Murphy PM. The CXC chemokines growth-regulated oncogene (GRO) alpha, GRObeta, GROgamma, neutrophil-activating peptide-2, and epithelial cell-derived neutrophil-activating peptide-78 are potent agonists for the type B, but not the type A, human interleukin-8 receptor. The Journal of biological chemistry. 1996; 271:20545–20550. [PubMed: 8702798]
54. Kammerer R, Buchner A, Palluch P, Pongratz T, Oboukhovskij K, Beyer W, et al. Induction of immune mediators in glioma and prostate cancer cells by non-lethal photodynamic therapy. PLoS One. 2011; 6:e21834. [PubMed: 21738796]
55. Bruyere C, Mijatovic T, Lonez C, Spiegl-Kreinecker S, Berger W, Kast RE, et al. Temozolomide-induced modification of the CXC chemokine network in experimental gliomas. International journal of oncology. 2011; 38:1453–1464. [PubMed: 21399866]

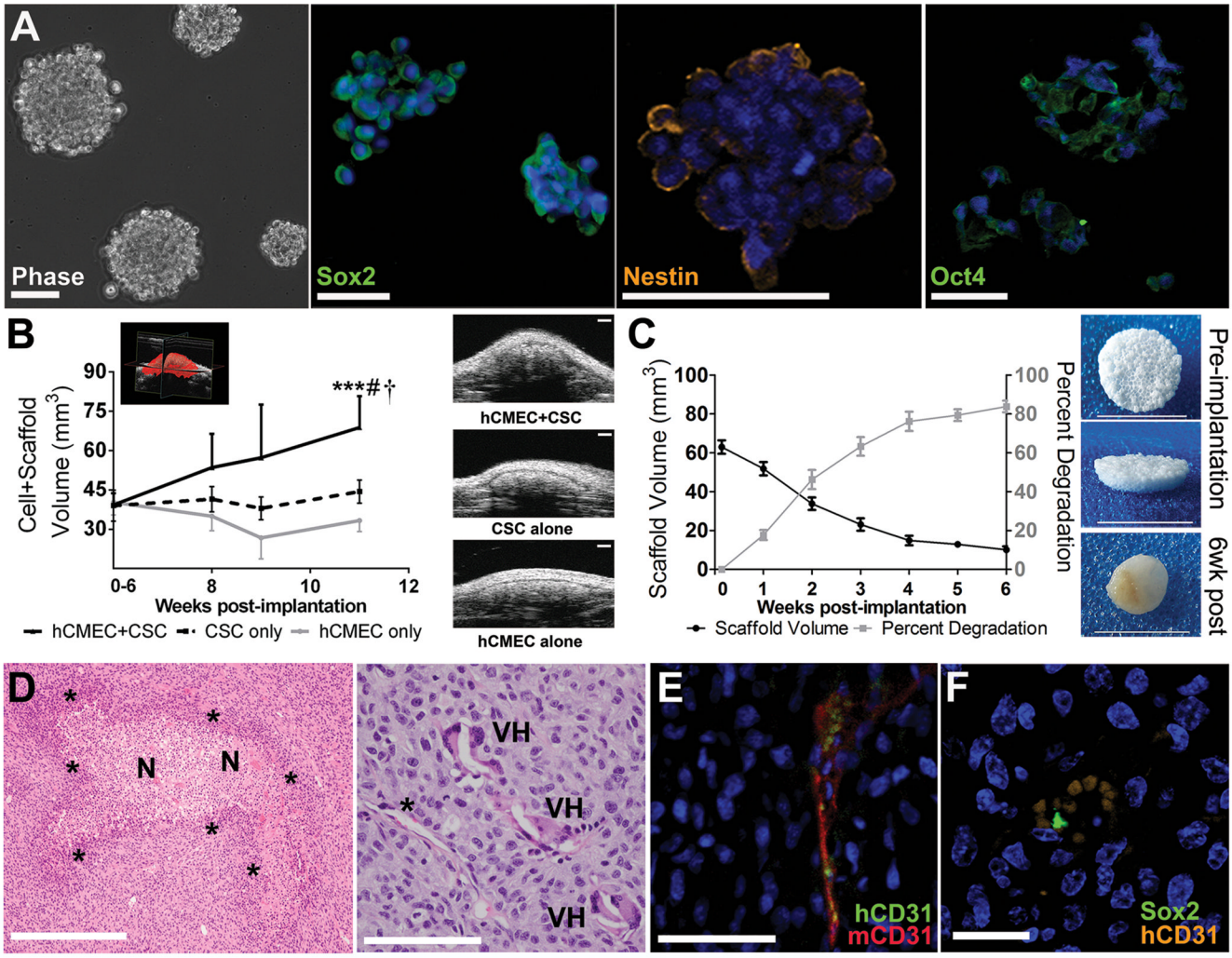

Figure 1. Brain ECs accelerate tumor formation by CSC-seeded 3-D polymeric scaffolds *in vivo*

A) Patient-derived CSCs form neurospheres when grown in stem cell culture conditions and robustly express stem cell markers Sox2, Nestin, and Oct4. Nuclear counterstain with DAPI. Scale bars: 50μm. B) Co-implantation of hCMECs with CSCs in porous PLG scaffolds accelerated tumor growth relative to CSC implantation alone as calculated from 3-D B-mode ultrasound images (inset) collected at weekly time points following implantation. Images show representative cross-sections of co-implanted and control groups 8 weeks following subcutaneous implantation. ***$p<0.001$ vs. hCMEC alone; #$p<0.01$ vs. CSC alone; †$p<0.05$ vs. CSC+hCMEC at 6 weeks. Scale bars: 1mm. C) Due to hydrolytic degradation the volume of blank control scaffolds was reduced markedly by 6 weeks as determined via longitudinal ultrasound measurements and confirmed following scaffold explantation. Scale bars: 1 cm. D) H&E stained cross-sections of tumors explanted after 8 weeks revealed clinical features of human GBM, including large necrotic (N) regions surrounded by pseudopalisades (*)(left panel) and vascular hypertrophy (VH) (right panel). (*) in right panel denotes non-hypertrophic vasculature for comparison. Scale bars: 500μm (left) and 100μm (right). E) Immunohistochemical analysis of co-implanted tumors using species-specific antibodies to the EC marker CD31 and DAPI counterstain as well as detection of blood cells within vessel lumens suggests that implanted hCMECs formed capillary structures that anastomosed with the mouse vasculature. Scale bar: 20μm. F)

Undifferentiated CSCs co-localized with hCMECs as detected by co-immunostaining for Sox2 and human CD31. Scale bar: 50μm.

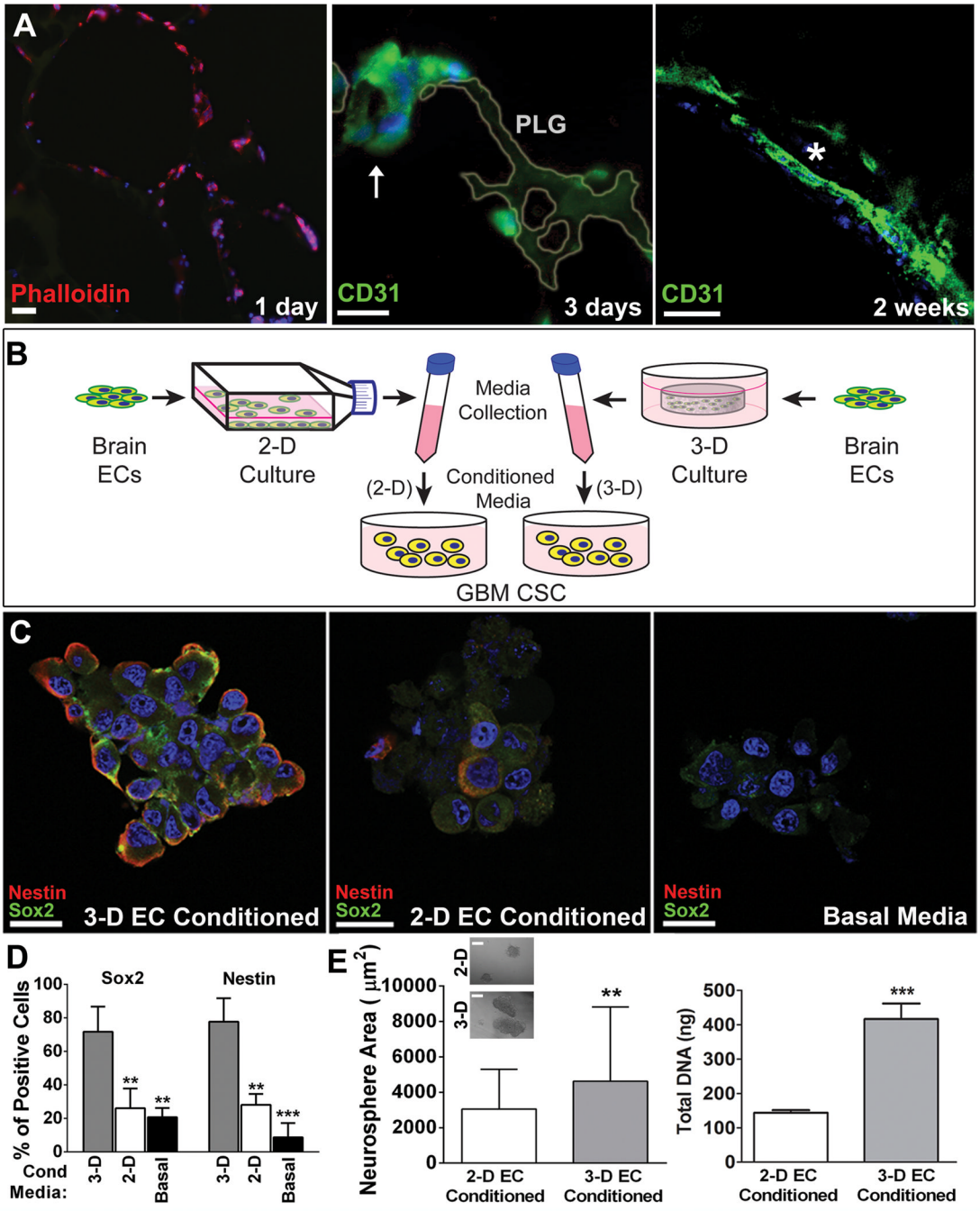

Figure 2. 3-D microenvironmental conditions stimulate EC secretion of molecules that support CSC functions *in vitro*

A) HCMECs seeded into PLG scaffolds readily adhered within scaffold pores and assembled into capillary-like structures by 3 days (middle panel, arrow) that matured into endothelial networks with lumenal architecture (*) by 2 weeks (right panel). DAPI counterstain. Scale bars: 20μm (phalloidin), 50μm (CD31). B) To evaluate microenvironment-dependent hCMEC paracrine signaling on GBM CSCs, conditioned media was collected from 2-D or 3-D hCMEC (EC) cultures, normalized to DNA content, and supplemented to CSC cultures. C) Representative images of CSC neurospheres following 5 days of culture with 3-D (left panel) or 2-D (middle panel)-conditioned hCMEC

media (or basal EC media, right) supplementation illustrates enhanced presence of stem cell markers Nestin (red) and Sox2 (green) in the presence of 3-D-derived soluble factors. DAPI counterstain. Scale bars: 20μm. D) Image analysis of Sox2- or Nestin-positive cells from CSC cultures supplemented with media from 2-D or 3-D EC conditioned media, or basal media. **p<0.01 or ***p<0.001 vs. 3-D EC conditioned media. E) Media collected from 3-D-cultured hCMECs enhanced neurosphere size (left, and inset images) and DNA content (right) relative to media obtained from 2-D hCMEC cultures. **p<0.01 vs. 2-D; ***p<0.001 vs. 2-D. Scale bar: 200μm.

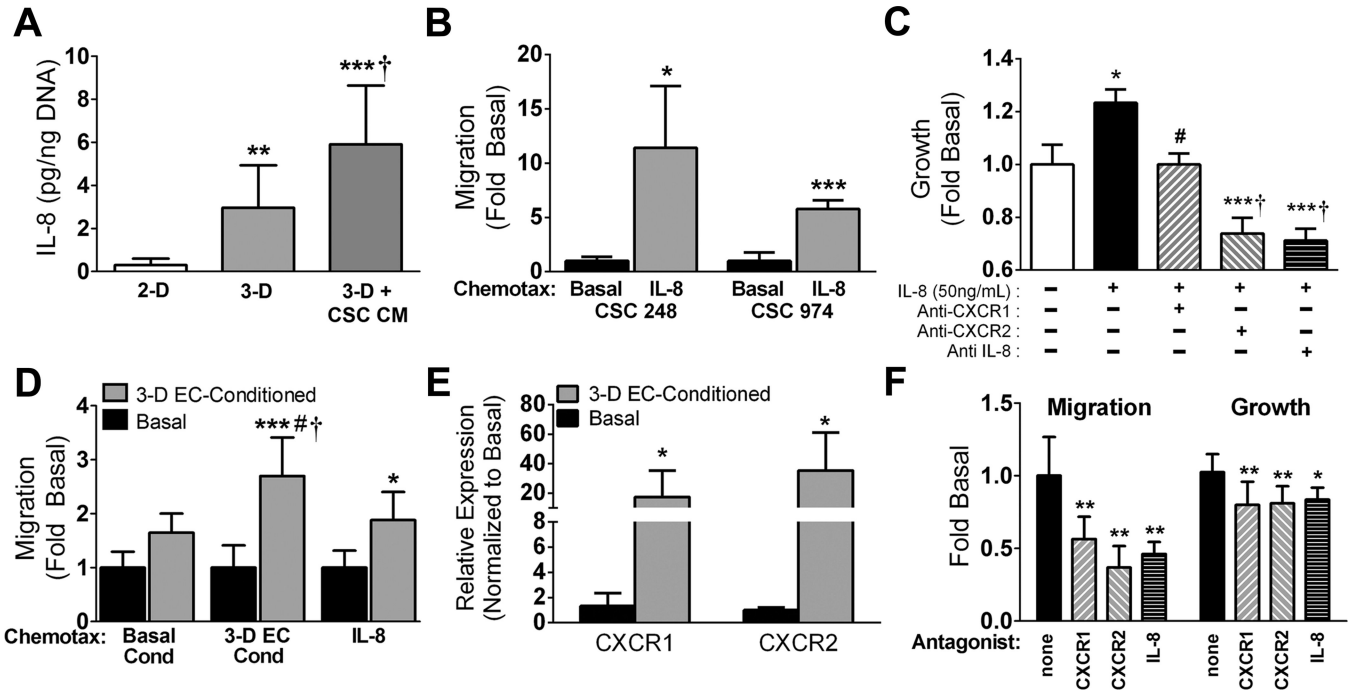

Figure 3. 3-D microenvironmental conditions enhance hCMEC-dependent CSC migration and growth in an IL-8-dependent manner

A) ELISA revealed that IL-8 secretion from hCMECs (normalized to DNA content) is enhanced in PLG scaffold cultures (3-D) vs. monolayers (2-D), and further increased when 3-D cultured cells are pre-conditioned with media collected from CSCs. **p<0.01 or ***p<0.001 vs. 2-D, † p<0.05 vs. 3-D. B) Transwell migration assays elucidated that IL-8 elevated migration of two separate CSC lines relative to basal control media. *p<0.05 or ***p<0.001 vs. media. C) DNA analysis 48 hours following IL-8 stimulation suggested that IL-8 enhanced CSC growth. Addition of CXCR1 antagonist antibodies abolished this effect, and antagonist antibodies to either IL-8 or CXCR-2 further attenuated growth to levels below control. *p<0.05 vs. basal, # p<0.05 or ***p<0.001 vs. CSC+IL-8, † p<0.01 vs. basal. D) Migration of CSCs towards 3-D hCMEC-secreted factors (3-D EC cond) or IL-8 was enhanced by pre-incubation of CSCs with media collected from 3-D cultured hCMECs (3-D EC-conditioned) relative to basal control media. Effects were more pronounced for migration towards 3-D EC media as compared to IL-8. *p<0.05 or ***p<0.001 vs. basal-conditioned CSCs of same chemotax; # p<0.05 vs. 3-D EC-Conditioned CSCs against basal cond chemotax; † p<0.05 vs. 3-D EC-Conditioned CSCs against IL-8 chemotax. E) Analysis of gene transcription via qPCR indicates that pre-conditioning of CSCs with conditioned media from 3-D hCMEC cultures upregulated (vs. basal media pre-conditioned) both cognate IL-8 receptors CXCR1 and CXCR2. *p<0.05 vs. basal-conditioned. F) The functional impacts of paracrine factors from 3-D hCMECs on CSC migration and growth rely upon IL-8 signaling: Transwell migration of 3-D hCMEC pre-conditioned CSCs towards IL-8 is robustly impaired with the addition of antagonist antibodies to CXCR1, CXCR2, and IL-8 (left). Elevated CSC growth imbued by similar pre-conditioning is attenuated with the presence of CXCR1, CXCR2, or IL-8 antagonist antibodies (right). *p<0.05 or **p<0.01 vs. control 3-D hCMEC-preconditioned CSCs.

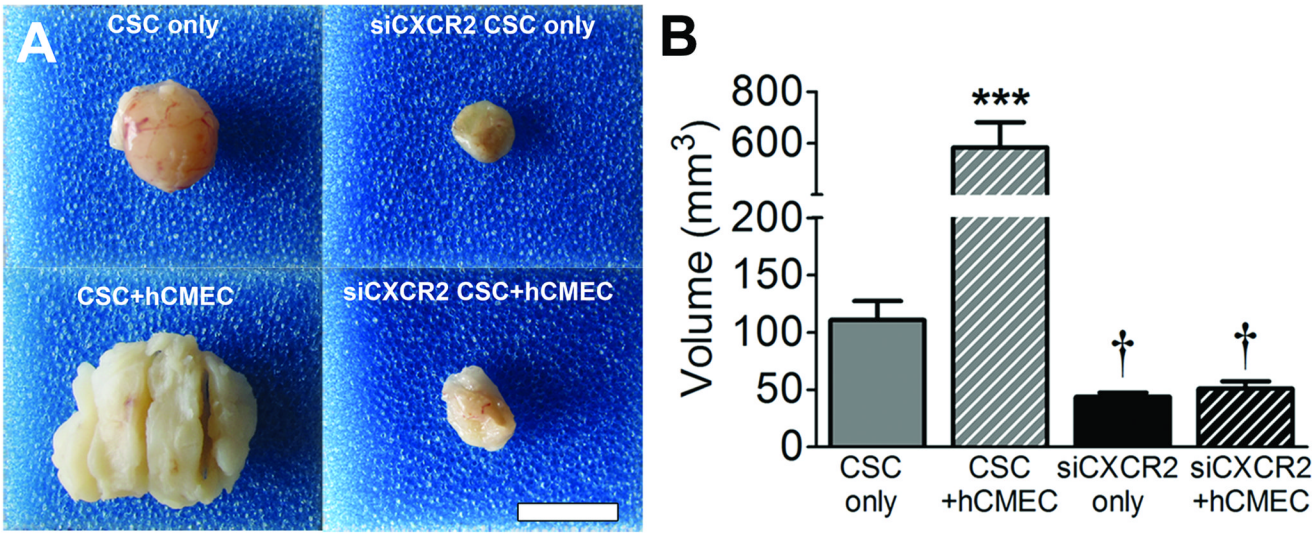

Figure 4. Inhibition of CSC CXCR2-signaling abolishes the stimulatory effects of hCMECs on tumorigenesis *in vivo*

A) Photographs of explanted tumors and B) 3-D *in vivo* ultrasound analysis of tumors 8 weeks following subcutaneous implantation of PLG scaffolds seeded with CSCs or sh-CXCR2 knocked-down CSCs alone or in combination with hCMECs confirmed a robust increase in tumor volume due to hCMEC co-implantation, which was abolished with CXCR2 knockdown. Scale bar: 1mm. ***$p<0.001$ or † $p<0.01$ vs. CSC only.